JOURNAL OF Applied Polymer SCIENCE

Molecular Design and Stabilization Mechanism of Acrylonitrile Bipolymer

Anqi Ju,[1] Shanyi Guang,[2] Hongyao Xu[1]

[1]College of Materials Science and Engineering & State Key Laboratory for Modification of Chemical Fibers and Polymer Materials, Donghua University, Shanghai 201620, China

[2]College of Chemistry, Chemical Engineering and Biology, Donghua University, Shanghai 201620, China

Correspondence to: H. Y. Xu (hongyaoxu@163.com)

ABSTRACT: In order to replace terpolymer with bipolymer, a bifunctional comonomer 3-aminocarbonyl-3-butenoic acid methyl ester (ABM) was synthesized for preparing poly(acrylonitrile-*co*-3-aminocarbonyl-3-butenoic acid methyl ester) [P(AN-*co*-ABM)] bipolymers as carbon fiber precursor. The structure and stabilization of P(AN-*co*-ABM) bipolymers were characterized by Fourier transform infrared spectroscopy, X-ray diffraction, and differential scanning calorimetry. The monomer reactivity ratios were calculated by the Fineman-Ross and Kelen-Tüdõs methods, and the results show that ABM displays higher reactivity than acrylonitrile. Two parameters $E_s = A_{1618cm}{}^{-1}/A_{2244cm}{}^{-1}$ and $SI = (I_0 - I_s)/I_0$ were defined to evaluate the extent of stabilization, and the activation energy (E_a) of the stabilization reactions were calculated by Kissinger and Ozawa methods. The results show that the P(AN-*co*-ABM) bipolymers exhibit significantly improved stabilization performance when compared with polyacrylonitrile (PAN) homopolymer, such as lower cyclization temperature, lower E_a, and larger extent of stabilization under the same conditions. Simultaneously, the rheological analysis shows that P(AN-*co*-ABM) possesses better spinnability than PAN. © 2013 Wiley Periodicals, Inc. J. Appl. Polym. Sci. 000: 000–000, 2013

KEYWORDS: copolymers; differential scanning calorimetry; X-ray; radical polymerization; thermal properties

Received 16 August 2012; accepted 9 November 2012; published online

DOI: 10.1002/app.38812

INTRODUCTION

Carbon fibers are predominantly manufactured from rayon, polyacrylonitrile (PAN), and pitch precursor fibers.[1] It is well known that the properties of the carbon fibers are mainly determined by the microstructure and mechanical properties of the precursor fibers.[2,3] Among all the available precursors, PAN fiber is one of the most successful and promising precursors for making high performance carbon fibers.[4] However, PAN homopolymer has hardly been used as a carbon fiber precursor because of its poor stabilization and spinnability. Therefore, PAN precursors are usually modified by incorporation of suitable comonomers into polymer chains to enhance its solubility, spinnability, hydrophilicity, and drawability, and especially to improve the stabilization of PAN, which plays an important role in the properties and quality of resulting carbon fiber.[5] Generally, acidic comonomers, such as acrylic acid (AA), methacrylic acid, and itaconic acid (IA), are often incorporated to reduce the cyclization temperature and improve the stabilization of PAN.[6,7] Neutral comonomers such as methyl acrylate (MA) and methyl methacrylate (MMA) are used to improve the solubility, drawability, and spinnability of PAN.[8] Thus, many terpolymers of acrylonitrile, such as P(AN-MA-IA), P(AN-MMA-IA), and P(AN-MA-AA), are used as carbon fiber precursors to improve the stabilization and spinnability of PAN.[9] However, it is very difficult to improve the stabilization as well as spinnability at the same time in PAN terpolymers because of the different reactivities of acidic comonomers and neutral comonomers. Generally, the reactivity of acidic comonomers is lower than that of neutral comonomers, which often results in less acidic comonomers incorporated into the polymer chains, so the initiation temperature of stabilization in the terpolymers is still rather high and the stabilization of PAN terpolymers is not improved significantly. If the amount of acidic comonomers in the feed ratio during polymerization increases, the resultant bipolymers will often exhibit lower molecular weight, which results in bad spinnability and poor performance of carbon fibers. The similar results have also been found in our previous research work.[10] In addition, the sequence composition in the terpolymers is difficult to be controlled. For these reasons, the terpolymers are not the best materials for carbon fiber precursor. In order to replace terpolymer with bipolymer, a bifunctional comonomer 3-aminocarbonyl-3-butenoic acid methyl ester (ABM) containing

both amide group and ester group was synthesized and used to prepare poly(acrylonitrile-*co*-3-aminocarbonyl-3-butenoic acid methyl ester) [P(AN-*co*-ABM)] binary copolymer in this article.

The copolymerization of acrylonitrile (AN) with comonomers can be done by various methods, such as solution, emulsion, aqueous suspension, and solvent-water suspension polymerization. Among these methods, the solution polymerization is the most favorable method, as it yields precursors with lower stabilization temperature and fewer molecular defects. In addition, the polymer solution can be converted directly to the spinning dope for fiber production.[11,12] Therefore, the solution polymerization has been used to prepare P(AN-*co*-ABM) bipolymers in this article. The copolymerization of AN with ABM was investigated in detail, and the thermal properties of P(AN-*co*-ABM) bipolymers with different monomer feed ratios were studied by FTIR, DSC, and XRD technologies. The spinnability of polymer solution has great effect on the physical properties of precursor fibers such as fineness, density, crystallinity, and drawability, which ultimately affects the mechanical properties of resultant carbon fiber. So, the spinnability of P(AN-*co*-ABM) was also investigated by rheological analysis.

EXPERIMENTAL

Materials

AN (analytical grade) was purchased from Shanghai Boer Chemical Reagent, Shanghai, China, and distilled twice before polymerization. Azodiisobutyronitrile (AIBN, analytical grade) was bought from Sinopharm Chemical Reagent, Shanghai, China, and recrystallized from methanol. Dimethyl sulfoxide (DMSO, analytical grade) was got from Shanghai Huadong Reagent Company, Shanghai, China and distilled by reduced pressure before use. IA, petroleum ether, methanol, benzene, thionyl chloride, chloroform, *N*,*N*-dimethylformamide, tetrahydrofuran, and benzoyl chloride (analytical grade) were purchased from Sinopharm Chemical Reagent, Shanghai, China, and used as received.

Synthesis of *β*-Methylhydrogen Itaconate

To a 100-mL round-bottomed flask was added IA (13.00 g, 100.00 mmol), methanol (14.20 mL, 350.00 mmol), and benzoyl chloride (0.50 mL, 4.30 mmol). The mixture was refluxed at 65°C for 0.5 h and then cooled to room temperature. The reaction mixture was distilled under reduced pressure to remove excess methanol and then followed by standing to get precipitation. The precipitation was recrystallized from benzene-petroleum ether (v/v = 1: 1).

White crystal, 84.52% yield. IR (KBr) υ_{max} cm^{-1}: 3004, 2955 (C—H), 1726, 1691 (C=O), 1636 (C=C), 1237, 1170 (C—O). ^{1}H-NMR (400 Hz, DMSO-d_6, RT, TMS) δ ppm: 12.616 (s, 1 H, COOH), 6.149 (d, J = 1.20 Hz, 1 H, CH_2=), 5.763 (d, J = 1.20 Hz, 1 H, CH_2=), 3.580 (s, 3 H, OCH_3), 3.336 (s, 2 H, CH_2).

Synthesis of ABM

β-Methylhydrogen itaconate (1.441 g, 10.00 mmol), chloroform (40.00 mL, 0.50 mol), thionyl chloride (1.10 mL, 15.00 mmol) and *N*,*N*-dimethylformamide (0.10 mL, 1.30 mmol) were added to a 150-mL three-necked flask. The mixture was refluxed at 70°C for 0.5 h and then cooled to room temperature. The reaction mixture was distilled under reduced pressure to remove excess thionyl chloride. After this, 40.00 mL of chloroform was added to the remaining residue. Then anhydrous ammonia was passed into the solution at 0°C until no more precipitate formed. The precipitate was filtered off and washed with chloroform (3 × 40 mL). The obtained chloroform solution was rotary evaporated at 40°C for 30 min to get crystalline residue.

Yellow crystal, 82.49% yield. IR (KBr) υ_{max} cm^{-1}: 3409, 3174 (N—H), 3000, 2953 (C—H), 1736, 1670 (C=O), 1645 (N—H), 1605 (C=C), 1174 (C—O). ^{1}H-NMR (400 Hz, DMSO-d_6, room temperature, tetramethylsilane) δ ppm: 7.594 (s, 1 H, $CONH_2$), 7.031 (s, 1 H, $CONH_2$), 5.893 (s, 1 H, CH_2=), 5.531 (d, 1 H, CH_2=), 3.587 (s, 3 H, OCH_3), 3.3329 (s, 2 H, CH_2).

Preparation of Polymers

Copolymerization of AN with different amounts of ABM was carried out in a three-necked flask at 60°C under nitrogen atmosphere using DMSO as the reaction medium. In the reaction system, the total monomer concentration was 25 wt %, and the concentration of AIBN was 0.8 wt % on the basis of total monomers. The reaction heat is dissipated sufficiently through good agitation, and the reaction was terminated by methanol after 24 h. The resultant mixture was poured into excess methanol with vigorous agitation to precipitate the polymer. The isolated precipitation was washed with methanol for three times and then dried at 60°C under vacuum to a constant weight.

Similar polymerization conditions were used to prepare the P(AN-*co*-ABM) bipolymers for determining the monomer reactivity ratios. The mole fraction of the comonomer ABM in the copolymerization system varied from 1 to 5 mol %, and the copolymerization was terminated at a low conversion of $\leq$10%.

Characterization

Viscosity average molecular weight (M_η) of the resultant polymers was measured by Ubbelolohde viscometer method at a constant temperature water bath of (50 ± 0.5)°C. The equation is depicted as follows:

$$[\eta] = 2.83 \times 10^{-4} M_\eta^{0.759}$$

where $[\eta]$ is the intrinsic viscosity calculated by linear extrapolation, and the measuring solvent is DMSO. The required polymer weight is 0.50 g in 50.00 mL DMSO.[8]

Proton nuclear magnetic resonance ^{1}H-NMR (400 MHz) spectra were recorded on a Bruker DMX-400 NMR spectrometer using DMSO-d_6 as a solvent at room temperature. Fourier transform infrared spectra (FTIR) of KBr disks were measured on a Thermo Nicolet 8700 FTIR spectrophotometer at room temperature; 32 scans were collected at a resolution of 1 cm^{-1}. Powder sample (1 mg) was mixed thoroughly with 200 mg of KBr and pelletized for FTIR characterization. The differential scanning calorimetry (DSC) curves were carried out on a TA instrument Modulated DSC 2910 under N_2 (40 mL min^{-1}). The sample weights used for DSC experiments were about 3-4 mg. Carbon (C), nitrogen (N), hydrogen (H), and oxygen (O) contents of P(AN-*co*-ABM) bipolymers were determined by a

Elementar Vario EL III elemental analyzer. Rheological measurements were recorded on a Haake RS150L Rotational rheometer at 70°C from 0 to 1000 s^{-1}; the polymer solutions were obtained by dissolving PAN polymer in the solvent and the concentration of them were 18 wt %. X-ray diffraction (XRD) patterns of powered samples were measured on a Rigaku D/max-2550 diffractometer between 3 and 50° at the rate of 3° min^{-1}. All the XRD measurements were carried out under the same conditions. The crystalline planar spacing d and crystallite size of the laterally order domains (L_c) were estimated by the Scherrer equation and Bragg equation respectively as follows:[13]

$$d = \lambda/\sin\theta \text{ and } L_c = k\lambda/B\cos\theta$$

where $\lambda = 0.154056$ nm is the wavelength of CuK_α X-ray, θ is the Bragg angle, B is the full-width at half-maximum intensity (FWHM) of the peak around $2\theta = 17°$, and K is a constant 0.89.

The crystallinity (CI) was determined by Bell and Dumbleton:[13]

$$CI = A_c/(A_c + A_a)$$

where A_c is the integral area of crystalline zone around $2\theta = 17°$ in XRD patterns, and A_a is the integral area of amorphous zone. A_c was calculated using straight line segments from $2\theta = 11°$ to $2\theta = 21°$ as the baseline, and the total integral area A ($A = A_a + A_c$) was evaluated using straight-line segments from $2\theta = 11°$ to $2\theta = 32°$ as the baseline.

For heat treatment, the powder samples were heated at constant temperature in an hot air oven with a temperature accuracy of 1°C for 30 min.

RESULTS AND DISCUSSION

Reactivity Ratio Studies

The molecular weight of ABM and AN are 143 and 53 g mol^{-1}, respectively. According to the mechanism of radical polymerization, presuming the end group effect on copolymer is ignored, the molar fraction of ABM in the resultant copolymer is calculated by the following equation:

$$[ABM] = \frac{C_O/(4\times 16)}{\frac{1-(C_O+143)/(4\times 16)}{53} + \frac{C_O}{4\times 16}} = \frac{53C_O}{64 - 90C_O}$$

where C_O is the oxygen content in the resultant copolymer. Therefore, the ratios of molar fraction of AN and ABM in the P(AN-*co*-ABM) bipolymers can be calculated from the element analysis results of oxygen, which are used by the Fineman-Ross[14] and Kelen-Tüdõs[15] methods to determine the monomer reactivity ratios.

According to the Mayo-lewis equation, the Fineman-Ross method is written as follows:

$$G = r_1 H - r_2$$

G and H are represented by

$$G = X(Y-1)/Y, \quad H = X^2/Y$$

where X and Y are the ratios of molar fraction of AN and ABM in the feed and in the resultant bipolymer, respectively:

Table I. Parameters for Solution Copolymerization of AN/ABM Under Low Conversion

X (mol mol^{-1})	Conversion (%)	O content in the bipolymers (wt %)	Y (mol mol^{-1})
99/1	6.29	1.785	48.03
98/2	6.47	3.45	23.55
97/3	6.05	4.85	15.97
96/4	6.14	6.255	11.78
95/5	5.93	7.495	9.38

$$X = [M_1]/[M_2], \quad Y = d[M_1]/d[M_2]$$

The plot of G versus H gives a straight line with the slope as r_1 and the intercept of the y-axis as r_2.

The linear relationship equations proposed by Kelen and Tüdõs are as follows:

$$\eta = (r_1 + \frac{r_2}{\alpha})\xi - \frac{r_2}{\alpha}$$

η and ξ are represented by

$$\eta = G/(\alpha + H), \quad \xi = H/(\alpha + H)$$

α is an arbitrary constant and represented by

$$\alpha = (H_m H_M)^{-1/2}$$

where H_m and H_M is the lowest and highest values calculated from the series of measurements. The plot of η versus ξ gives a straight line. The extrapolation of the line to $\xi = 1$ gives r_1 and to 0 gives $-r_2/\alpha$.

The parameters for copolymerization of AN with ABM under low conversion are shown in Table I. On the basis of Table I, the monomer reactivity ratios are calculated by the Fineman-Ross and Kelen-Tüdõs methods. The reactivity ratios of ABM calculated by Fineman-Ross and Kelen-Tüdõs methods are 1.62 and 1.48, respectively, and the reactivity ratios of AN calculated by these two method are both 0.48. It can be found out that the reactivity ratios calculated by these two methods show good agreement and the reactivity ratio values of ABM are larger than that of AN, indicating ABM has higher reactivity than AN. Hence, the propagating radicals ~AN· and ~ABM· have a preference to the comonomer ABM and the probability of ABM entering into the polymer chains is higher than that of AN. From the above results, it is expected that the content of ABM will be richer in the resultant copolymer than in the feed, and the evidence can be found in following element analysis (Molecular Weight and Elemental Analysis Studies section).

Molecular Weight and Elemental Analysis Studies

The effect of monomer feed ratio on the conversion of polymerization and molecular weight of P(AN-*co*-ABM) are shown in Figure 1. It is easy to see that both the conversion of

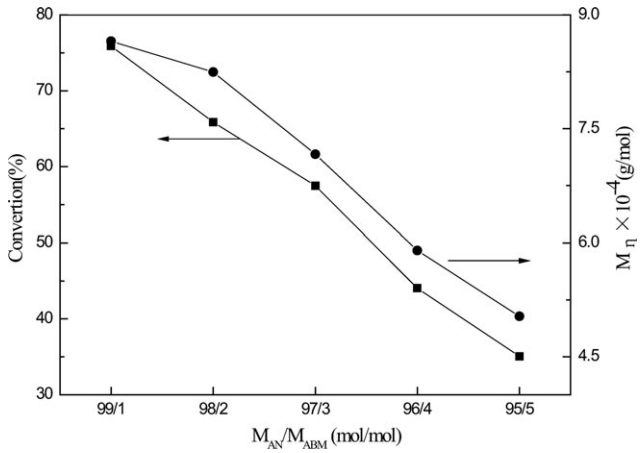

Figure 1. Effect of monomer feed ratio on the conversion of polymerization and molecular weight.

polymerization and molecular weight of P(AN-*co*-ABM) reduce with the increasing of ABM amounts in the feed. This may be attributed to the large volume of ABM molecules, which counteracts the growth of polymer chains and reduces the conversion of polymerization and molecular weight.[16] It is proved that the molecular weight of PAN polymers has great effect on the performance of resulting carbon fiber, so the amounts of bifunctional comonomer ABM in the feed should be well controlled to get high molecular weight P(AN-*co*-ABM). As shown in Figure 1, the amount of ABM in the feed should be controlled less than 2.0 mol % based on total monomers in order to prepare high molecular weight P(AN-*co*-ABM) as carbon fiber precursor.

The element analysis results of P(AN-*co*-ABM) bipolymers with different monomer feed ratios are shown in Table II. Obviously, the oxygen (O) element in P(AN-*co*-ABM) bipolymers is provided by the bifunctional comonomer ABM. As shown in Table II, the O content in the resultant bipolymers increases with the increasing of ABM amounts in the feed, suggesting that more ABM are incorporate into the PAN polymer chains. It is known that the hydrogen (H) content is richer in ABM (6.33 wt %) than in AN (5.69 wt %), so the H content of in the resultant bipolymers increases with the increasing of ABM amounts in the feed. While the contents of carbon (C) and nitrogen (N) are lower in ABM than in PAN, resulting in the decrease of C and N content in the P(AN-*co*-ABM) bipolymers as shown in Table II. In addition, the content of O element in the feed (O_f) is also shown in Table II. The O content is richer in the resultant bipolymers than in the feed, indicating that the ABM content in the resultant polymers is richer, which confirms the above results (Reactivity Ratio Studies section) that ABM has higher reactivity than AN.

FTIR Studies

The FTIR spectra of original PAN homopolymer and P(AN-*co*-ABM) bipolymers with different monomer feed ratios are shown in Figure 2(A). As shown in Figure 2(A), the bands at 1729 and 1677 cm^{-1}, which are assigned to stretching vibration of C═O and bending vibration of N─H in comonomer ABM,[17,18] respectively, appear in the spectra of P(AN-ABM) bipolymers, suggesting that the bifunctional comonomer ABM has copolymerized with AN successfully. Furthermore, the intensity of bands at 1729 and 1677 cm^{-1} becomes stronger with the increasing of ABM amounts in the feed, indicating the increase of ABM content in the resultant bipolymers, which is consistent with the above element analysis results (Molecular Weight and Elemental Analysis Studies section). It is also found that the intensity of bands at 2244 cm^{-1} assigned to stretching vibration of C≡N[17] does not show obvious changes in all the polymers, suggesting the presence of long uninterrupted sequences of AN units in the polymer chains.[19] The intensity of the bands at 2939 cm^{-1} assigned to the C─H stretching vibration of CH, CH_2, and CH_3[20,21] and the bands at 1450 and 1357 assigned to C─H vibrations of different modes almost keep unchanged in all polymers.

The FTIR spectra of PAN homopolymer and P(AN-*co*-ABM) bipolymers with different monomer feed ratios stabilized at 200°C in air for 30 min are shown in Figure 2(B). Of particular interest are the bands at 2244 cm^{-1} assigned to stretching vibration of C≡N and the bands at 1618 cm^{-1} assigned to stretching vibration of C═N conjugated with C═C. As we all know, the cyclization reactions turn ─C≡N groups into ─C═N─ structure and the dehydrogenation reactions convert ─CH_2─CH_2─ structure into ─CH═CH─ structure, so the intensity changes of bands at 2244 and 1618 cm^{-1} can be used to evaluate the extent of stabilization. A parameter (E_s) is defined as follows to evaluate the extent of stabilization:

$$E_s = A_{1618cm^{-1}}/A_{2244cm^{-1}}$$

where A is the absorbance intensity defined as $A = \log(T_0/T)$, T_0 and T are the transmittances at baseline and maximum, respectively. According to Lambert-Beer's law: $A = abc$, where a is the molar absorption coefficient, b is the thickness of the KBr pellet (cm), and c is the mole concentration of sample solution (mol cm^{-1}). As the absorbance intensities of bands at 1618 and 2244 cm^{-1} are determined by the same KBr pellet, namely, with the same value of b, the ratio of absorbance intensity of these two bands is approximately equal to the ratio of contents of the generated C═N and C═C groups to the residual C≡N groups.[22] Thus the value of E_s can be use to represent the extent of stabilization. The molar ratio of ABM to AN in the P(AN-*co*-ABM) bipolymers with different monomer feed ratios can be

Table II. Elemental Analysis Results of PAN and P(AN-*co*-ABM) Bipolymers with Different Feed Monomer Ratios

AN/ABM (mol mol^{-1})	C	H	N	O	O_f
100/0	67.81	5.72	26.47	0	0
99/1	65.74	5.79	25.02	3.45	0.89
98/2	64.18	5.838	24.75	5.232	1.75
97/3	64.15	5.846	23.62	6.384	2.58
96/4	63.56	5.91	22.91	7.62	3.39
95/5	62.97	5.913	22.78	8.337	4.17

O_f: O content in the feed.

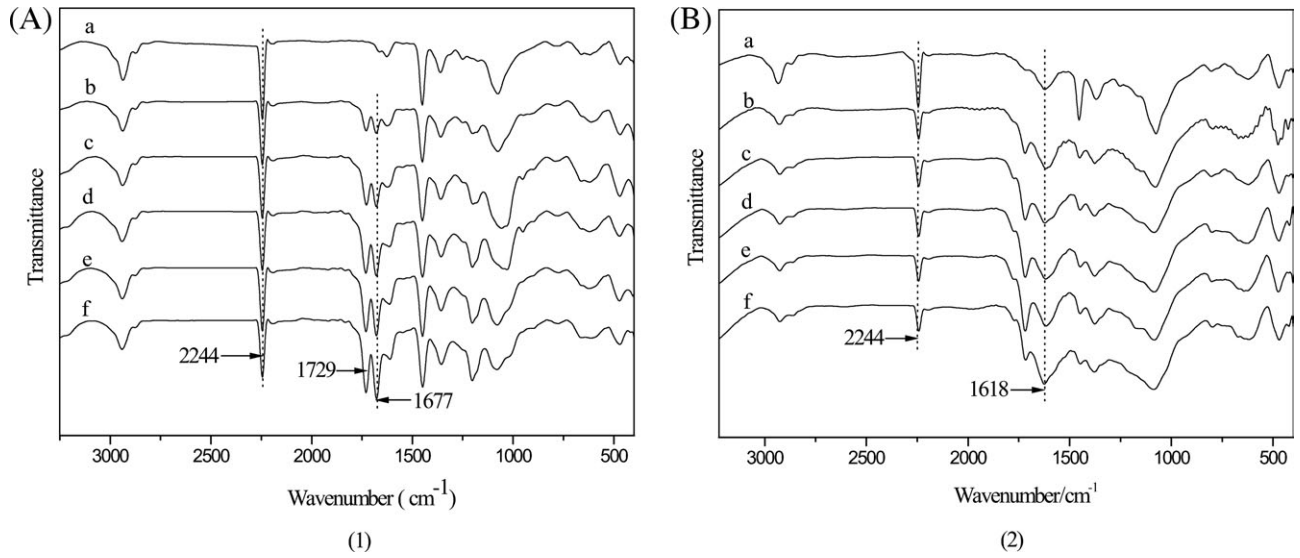

Figure 2. FTIR spectra of PAN and P(AN-*co*-ABM) bipolymers (A) original and (B) stabilized 200°C for 30 min: (a) PAN, (b) AN/ABM = 99/1 (mol mol^{-1}), (c) AN/ABM = 98/2 (mol mol^{-1}), (d) AN/ABM = 97/3 (mol mol^{-1}), (e) AN/ABM = 96/4 (mol mol^{-1}), and (f) AN/ABM = 95/5 (mol mol^{-1}).

calculated from the element analysis of O content in Table II, so the plot of E_s versus molar ratio of ABM to AN in P(AN-*co*-ABM) bipolymers is shown in Figure 3. As shown in Figure 3, the E_s values become larger with the increasing of ABM content in the P(AN-*co*-ABM) bipolymers, suggesting the incorporation of ABM into PAN polymer chains can improve the extent of stabilization effectively and the more the better. It is widely accepted that the cyclization of nitrile groups in PAN homopolymer can only be initiated through a free radical mechanism (Scheme 1). While the cyclization in P(AN-*co*-ABM) bipolymers can be initiated through both a radical mechanism (Scheme 1) and an ionic mechanism (Scheme 2).[23] As shown in Scheme 2, the amino nitrogen of acylamino (—$CONH_2$) in ABM can make a nucleophilic attack on the carbon atom of adjacent nitrile groups and induces molecules to cyclize, which can initiate the cyclization of nitrile groups successfully at a low temperature and improve the stabilization of P(AN-*co*-ABM) significantly.

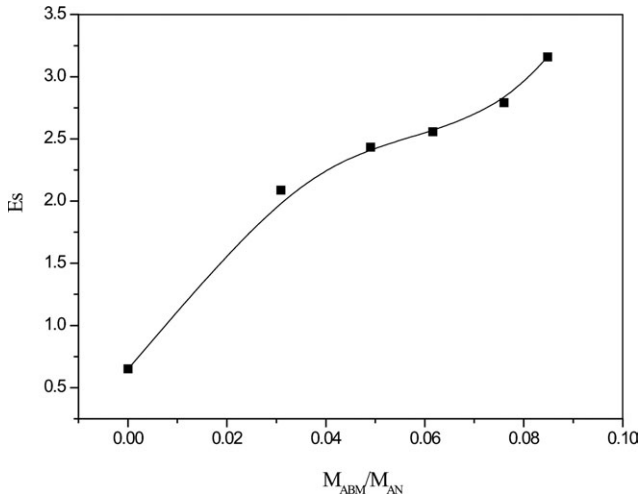

Figure 3. Effect of molar ratio of ABM and AN in P(AN-*co*-ABM) on the extent of stabilization (E_S).

XRD Studies

XRD patterns of original PAN homopolymer and P(AN-*co*-ABM) bipolymers are shown in Figure 4(A). The strongest diffraction peak at about $2\theta = 17°$ is attributed to the (100) crystalline plane of the pseudohexagonal cell.[23] At the same time, a weak diffraction peak at about $2\theta = 29°$ is attributed to the (101) crystalline plane of the pseudohexagonal cell.[24] XRD patterns of PAN polymers were processed by Origin 7.5 software to analyze the peak center, peak area, peak intensity and the FWHM of peak about $2\theta = 17°$. Based on the above results, the corresponding acrystalline planar spacing d, crystallite size L_c, and crystallinity CI were calculated. All the data are summarized in Table III. It is obvious that the peak intensity, peak area, and crystallinity CI of P(AN-*co*-ABM) bipolymers were smaller than that of PAN homopolymer as shown in Table III. Furthermore, the peak area, peak intensity, and CI values of P(AN-*co*-ABM) bipolymers decrease with the increasing of ABM contents in the resultant P(AN-*co*-ABM) bipolymers. The possible reason is that the incorporation of ABM into PAN polymer chains blocks the interactions between intermolecular C≡N groups, which enhances the activity of chain segments and reduces the crystallinity of P(AN-*co*-ABM). In addition, all the L_c values of P(AN-*co*-ABM) bipolymers are larger than that of PAN homopolymer, which may attribute to the large volume of ABM. As shown in Figure 4(A), the peak center about $2\theta = 17°$ hardly moves with the increasing of ABM content in P(AN-*co*-ABM) bipolymers, so the d values of PAN and P(AN-*co*-MHI) bipolymers almost keep unchanged.

XRD patterns of PAN and P(AN-*co*-ABM) bipolymers stabilized at 200°C for 30 min are shown in Figure 4(B). The stabilization of PAN polymers is a process converting linear structure into ladder structure. It has been reported that the structural changes

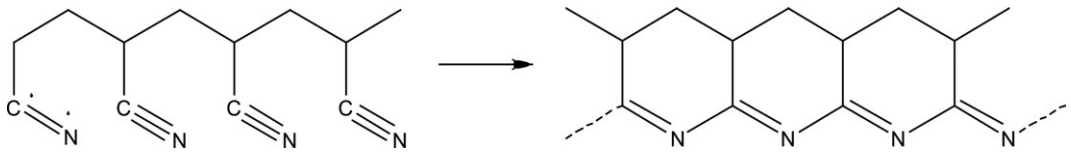

Scheme 1. Cyclization in PAN initiated through a free radical mechanism.

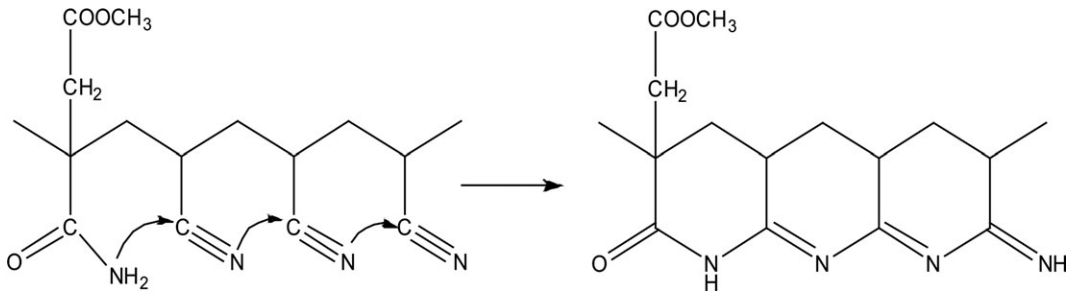

Scheme 2. Cyclization in P(AN-*co*-ABM) bipolymers initiated through an ionic mechanism.

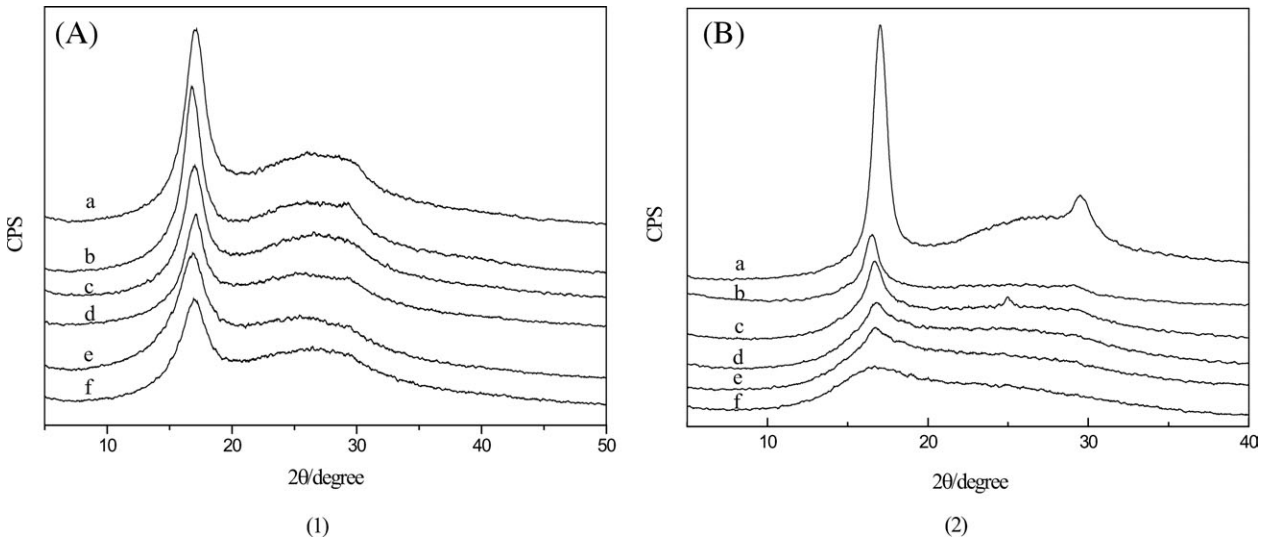

Figure 4. XRD patterns of PAN and P(AN-*co*-ABM) bipolymers (A) original and (B) stabilized 200°C for 30 min: (a) PAN, (b) ABM/AN = 0.0310 (mol mol^{-1}), (c) ABM/AN = 0.0491 (mol mol^{-1}), (d) ABM/AN = 0.0617 (mol mol^{-1}), (e) ABM/AN = 0.0761 (mol mol^{-1}), and (f) ABM/AN = 0.0848 (mol mol^{-1}).

during the stabilization agree well with the intensity changes of the peak about $2\theta = 17°$.[25] So the intensity changes about $2\theta = 17°$ can be used to evaluate the extent of stabilization, the equation is expressed as follows:[23]

$$SI = (I_0 - I_s)/I_0$$

where I_0 is the intensity of the peak about $2\theta = 17°$ from the original polymer, and I_s is the intensity of the peak about $2\theta =$

Table III. XRD Analysis Results of PAN and P(AN-*co*-ABM) Bipolymers Corresponding to Figure 4(A)

ABM/AN (mol mol^{-1})	Peak center (°)	Peak intensity (CPS)	Peak area	FWHW (°)	*d* (nm)	L_c (nm)	CI (%)
0 (PAN)	17.18	5345	37,771	0.926	0.5216	8.8798	50.24
0.0310	16.80	5036	29,217	0.848	0.5330	9.6770	47.69
0.0491	17.06	3450	22,951	0.917	0.5251	8.9612	46.11
0.0617	17.14	3171	19,456	0.777	0.5227	10.5803	45.19
0.0761	16.90	2391	18,944	0.907	0.5299	9.0523	44.09
0.0848	16.94	2194	18,336	0.874	0.5287	9.3960	40.54

Table IV. XRD Analysis Results of PAN and P(AN-*co*-ABM) Bipolymers Corresponding to Figure 4

ABM/AN (mol mol^{-1})	Peak center (°)	Peak intensity I_0 (CPS)	Peak intensity I_s (CPS)	SI (%)
0.0000	17.03	5345	11,415	−113.56
0.0310	16.53	3572	2863	19.85
0.0491	16.69	3529	2582	26.83
0.0617	16.82	2338	1367	41.53
0.0761	16.72	1050	609	42.12
0.0848	16.70	769	443	42.39

17° from the polymer stabilized at 200°C for 30 min. SI values determined by the above equation are listed in Table IV. The (100) peak intensity of PAN homopolymer stabilized at 200°C is higher than that of original PAN homopolymer and the SI value is negative, which can be elucidated by further crystallization in the PAN homopolymer. From the following DSC analysis (DSC Studies section), it is known that the stabilization reactions of PAN homopolymer have not yet started significantly at 200°C, because the cyclization of nitrile groups in PAN homopolymer can only be initiated through a free radical mechanism at a high temperature about 244°C. However, the energy provided by heating is enough to break the boundaries between crystalline zones and amorphous zones,[23] which results in further crystallization of PAN and increase in (100) peak intensity, so the SI value of PAN is negative. As shown in Table IV, the SI values of P(AN-*co*-ABM) bipolymers become larger with the increasing of ABM contents in P(AN-*co*-ABM) bipolymers, indicating the increase of the extent of stabilization in P(AN-*co*-ABM) bipolymers, which further supports that the incorporation of ABM into PAN polymer chains can improve the stabilization of P(AN-*co*-ABM) effectively and the more the better.

DSC Studies

Figure 5 shows the DSC curves of PAN homopolymer and P(AN-*co*-ABM) bipolymers heated at 10°C min^{-1} from ambient temperature to 400°C under N_2 (40 mL min^{-1}). The parameters obtained from the exotherms, including the temperature of initiation (T_i), the temperature of termination (T_f) and their difference ($\Delta T = T_f - T_i$), the first peak temperature (T_{p1}, the peak at low temperature), the second peak temperature (the peak at high temperature), the heat release (ΔH), and the rate of heat release ($\Delta H/\Delta T$), are listed in Table V.

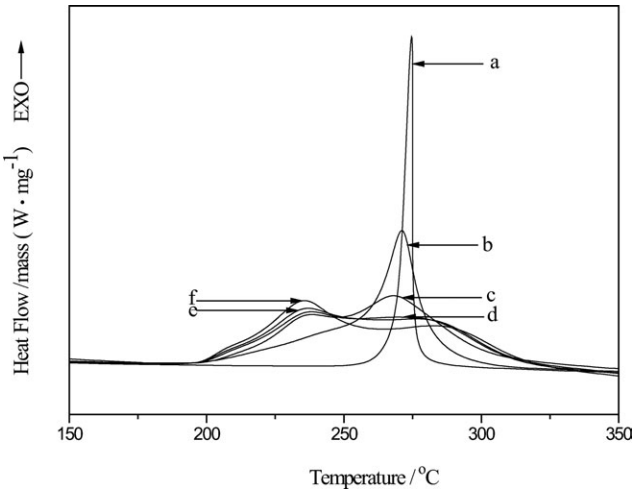

Figure 5. DSC curves of PAN and P(AN-*co*-ABM) bipolymers heated at 10°C min^{-1} under N_2 atmosphere: (a) PAN, (b) ABM/AN = 0.0310 (mol mol^{-1}), (c) ABM/AN = 0.0491 (mol mol^{-1}), (d) ABM/AN = 0.0617 (mol mol^{-1}), (e) ABM/AN = 0.0761 (mol mol^{-1}), and (f) ABM/AN = 0.0848 (mol mol^{-1}).

The DSC curves of PAN polymers were measured under N_2 atmosphere and no oxidative reactions occurred during this process, so the exothermic peaks in DSC curves are attributed to the cyclization reactions. As shown in Figure 5, there is only one exothermic peak in PAN homopolymer and the cyclization reactions of PAN homopolymer can only be initiated through a free radical mechanism at a high temperature about 244°C,[26] causing a large amount of heat to be released at the same time, which can break the molecular chains and further results in defect in the resultant carbon fibers. Whereas in P(AN-*co*-ABM) bipolymers, the cyclization reactions can be initiated through both a radical mechanism and an ionic mechanism,[27] so there are two exothermic peaks in DSC curves and the initiation temperature of cyclization has been lowered to about 185°C. The low exothermic peak (peak 1) is assigned to cyclization reactions initiated through an ionic mechanism, which broadens the exothermic peak and avoids centralized heat release. It is surprising to see that the area of peak 1 increases with the increasing of ABM content in P(AN-*co*-ABM) bipolymers, indicating that more cyclization reactions were initiated by ABM through an ionic mechanism increases. As shown in Table V, the T_i of P(AN-*co*-ABM) bipolymers is much lower than that of PAN homopolymer and becomes lower with the increasing of ABM

Table V. Parameters for DSC Curves of PAN and P(AN-*co*-MHI) Bipolymers Measured under N_2 Atmosphere

ABM/AN (mol mol^{-1})	T_i (°)	T_{p1} (°C)	T_{p2} (°C)	T_f (°C)	ΔT (°C)	ΔH (J g^{-1})	$\Delta H/\Delta T$ (J g^{-1}°C^{-1})
0.0000	244.16	278.99		303.11	58.95	2004.67	34.01
0.0310	191.39	271.11		329.28	137.89	2021.26	14.66
0.0491	190.83	238.25	267.98	335.44	144.61	2311.10	15.98
0.0617	190.32	238.08	270.28	351.60	161.28	2241.59	13.90
0.0761	188.38	237.11	276.30	354.52	166.14	2380.50	14.32
0.0848	184.20	235.47	282.34	360.00	175.8	2281.07	12.97

Applied Polymer SCIENCE

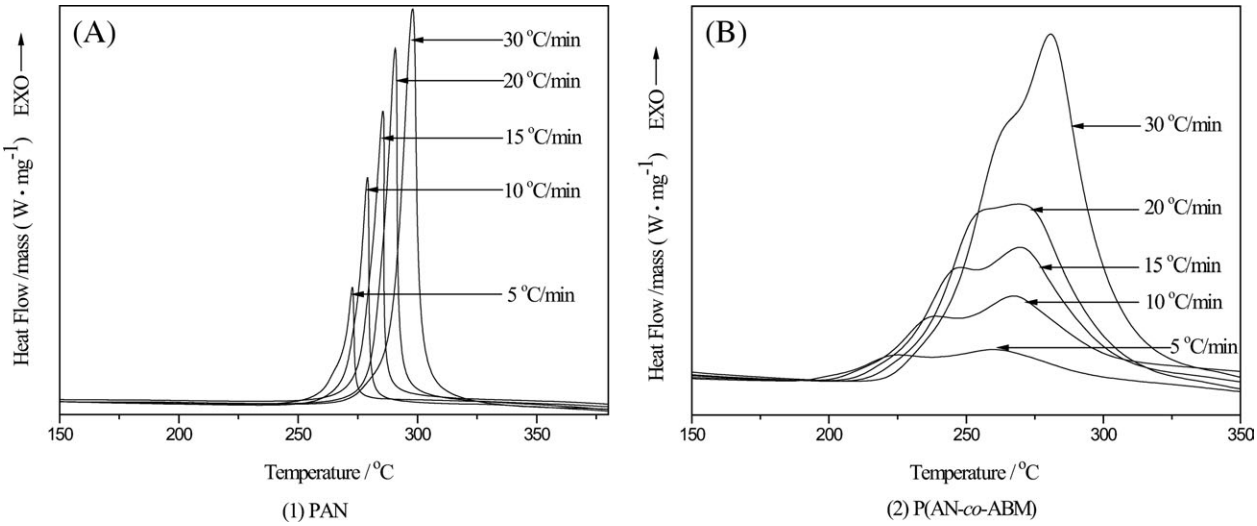

Figure 6. DSC curves of PAN (A) and P(AN-*co*-ABM) (B) heated at different rates.

content in P(AN-*co*-ABM) bipolymers, suggesting an easier initiation of cyclization reactions in P(AN-*co*-ABM) bipolymers than in PAN homopolymer. For the same reason, the T_{p1} exhibits the same tendency as T_i. The initiation temperature of the terpolymers, such as P(AN-MA-AA), P(AN-MA-IA), and P(AN-MMA-IA), are about 225°C, which is much higher than that of P(AN-*co*-ABM) bipolymers (ca. 185°C), hinting that P(AN-*co*-ABM) bipolymers showed better stabilization than terpolymers.[9] Even the content of carboxyl group in the P(AN-MMA-IA) is three times of acylamino group in P(AN-*co*-ABM) prepared in this work, the initiation temperature is still 215°C much higher than that of P(AN-*co*-ABM). This phenomenon was also observed in Devasia's work.[11] Thus, it can be concluded that the P(AN-*co*-ABM) bipolymers are much more advantageous than terpolymers in improving the stabilization of PAN. As shown in Table V, PAN homopolymer has the smallest ΔT and the largest $\Delta H/\Delta T$, implying the heat release in PAN homopolymer during stabilization is concentrative and expeditious. The incorporation of ABM into PAN polymer chains slows the rate of heat release efficiently, as evidenced from the larger ΔT and smaller $\Delta H/\Delta T$ in the P(AN-*co*-ABM) bipolymers. Furthermore, ΔT has a tendency to become larger with the increasing of ABM content in P(AN-*co*-ABM) bipolymers, whereas $\Delta H/\Delta T$ has a tendency to become smaller. It can be concluded that the incorporation of comonomer ABM into PAN polymer chains can lower the initiation temperature of cyclization and moderates heat release during stabilization, which is beneficial to making high performance carbon fiber.

Evaluation of Activation Energy (E_a) of Stabilization Reactions

Figure 6 shows DSC curves of PAN homopolymer and P(AN-*co*-ABM) bipolymer with ABM/AN = 0.0491 (mol mol^{-1}) heated at different rates (5, 10, 15, 20, 30°C min^{-1}) from ambient temperature to 400°C under N_2 (40 mL min^{-1}). As the heating rate increases, the exotherms wholly shift to higher temperature and the exothermic peaks become stronger for both PAN homopolymer and P(AN-*co*-ABM) bipolymer. The E_a of the cyclization reactions were determined by Kissinger method[28] and Ozawa method.[29] These two methods are mostly used to calculate E_a in literatures, because they can be used to quantify E_a without any prior knowledge of reaction mechanism but just requiring a series of DSC curves heated at different rates. It is found that the maximum peak of DSC (T_m) used to evaluate E_a shows a regular increase with the increasing of heating rate (ϕ).

Kissinger's method uses an equation as follows:[28]

$$-\frac{E_a}{R}=\frac{d\left[\mathrm{In}(\varphi/T_m^2)\right]}{d(1/T_m^2)}$$

E_a was calculated from the slope of the linear plot of $\ln(\phi/T_m^2)$ versus $1000/T_m$ as shown in Figure 7(A).

Ozawa's method makes use of the following equation:[29]

$$-\frac{E_a}{R}=2.15\frac{d(\log\varphi)}{d(1/T_m)}$$

E_a was calculated from the slope of the linear plot of $\log\phi$ versus $1000/T_m$ as shown in Figure 7(B).

The E_a of cyclization reactions of P(AN-*co*-ABM) bipolymers with ABM/AN = 0.0310, 0.0617, 0.0761, and 0.0848 (mol mol^{-1}) were also calculated by Kissinger and Ozawa methods. All the calculated results of E_a are listed in Table VI. It is found that the values of E_a calculated from Kissinger and Ozawa methods are almost the same. The DSC curves were obtained under N_2 atmosphere, so only cyclization reactions occurred during this process. The E_a of cyclization reactions in PAN homopolymer is about 168 kJ mol^{-1}, while in P(AN-*co*-ABM), the E_a has been split into two parts. The first part assigned to the ionic cyclization reactions is calculated from the first exothermic peak and the E_a is about 94 kJ mol^{-1}. The second part is calculated from the second exothermic peak and the is E_a about 190 kJ mol^{-1}, which is assigned to the radical cyclization

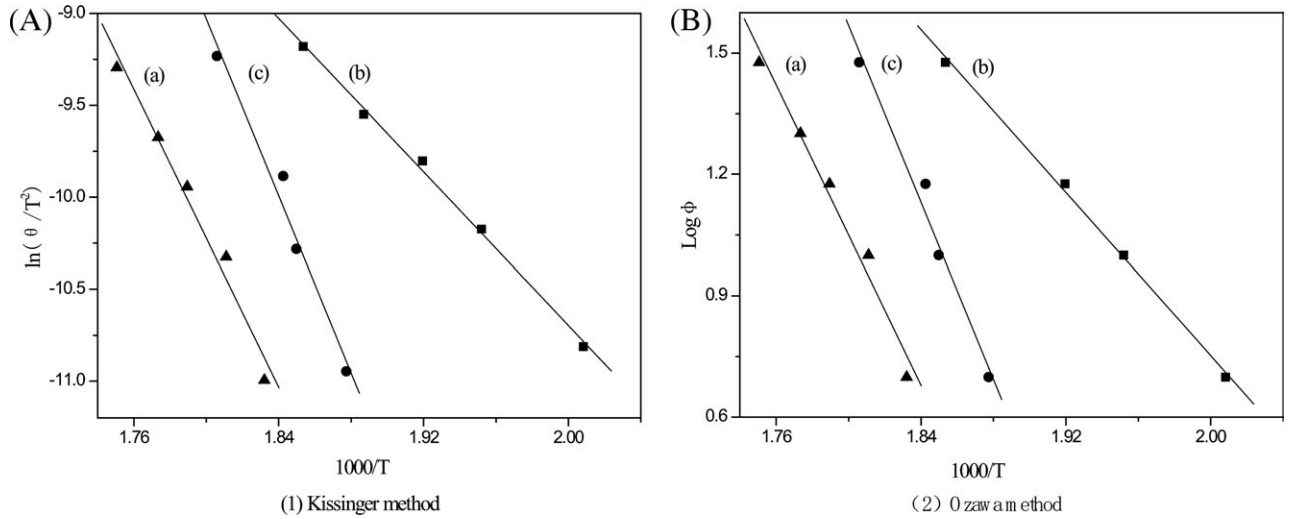

Figure 7. Kissinger method (A) and Ozawa method (B) used to quantify E_a: (a) PAN, (b) Peak 1 of P(AN-*co*-ABM), (c) Peak 2 of P(AN-*co*-ABM).

reactions. Obviously, the E_a of cyclization reactions has been significantly reduced by the incorporation of ABM into PAN chains, which is mainly due to the change of cyclization mechanism caused by ABM.[27] The decrease of E_a in P(AN-*co*-ABM) bipolymers confirms that the cyclization of nitrile groups has been promoted by the bifunctional comonomer ABM, which is beneficial to stabilization of PAN.

Rheological Analysis of PAN/DMSO and P(AN-*co*-ABM)/DMSO Solutions

The flow curves of PAN ($M_\eta = 8.79\times10^4$ g mol^{-1}) homopolymer and P(AN-*co*-ABM) bipolymer with ABM/AN = 0.0310 (mol mol^{-1}) ($M_\eta = 8.65\times10^4$ g mol^{-1}) in DMSO solutions at 70°C are shown in Figure 8. Both PAN/DMSO and P(AN-*co*-ABM)/DMSO solutions show shear thinning at high shear rates, which is explained by the breakage of entangled networks and the shear alignment of molecules.[30] The entanglement points are formed between molecules because of the intermolecular van der Waals forces, it can be distorted in one place and rearranged in another place due to the random thermal motion of polymer chains. The density of entanglement points depends on the external conditions such as temperature, shear rate, etc. At the low sheer rate, the destroyed entanglement points have enough time to rearrange and the density of entanglement points is unchanged, so the apparent viscosity keeps unchanged. With the increasing of shear rate, the rearranging rate of entanglement points cannot catch up with the destroying rate, so the density of entanglement points decreases, which results in the decrease of apparent viscosity. On the other hand, the molecular chains of polymers are aligned in the direction of flow, which can also cause the decrease of apparent viscosity.[31] In addition, the η_a value of P(AN-*co*-ABM) is smaller than that of PAN as shown in Figure 8, which is attributed to the decrease of intermolecular forces caused by the incorporation of MHI into PAN chains.

The structural viscosity index ($\Delta\eta$) represents the degree of structurization of polymer solution and can be calculated by the following equation:[32]

$$\Delta\eta = -\left[\frac{d1g\eta_a}{d(\dot{\gamma}^{1/2})}\right] \times 100$$

where η_a is the apparent viscosity of polymer solution and $\dot{\gamma}$ is the shear rate. It has been reported that the $\Delta\eta$ can be used as an indication of spinnability.[32,33] The smaller the $\Delta\eta$ value is, the better the spinnability is. The calculated $\Delta\eta$ of PAN/DMSO and P(AN-*co*-ABM)/DMSO solution system are 6.61 and 4.74, respectively, indicating that P(AN-*co*-MHI) possesses better spinnability than PAN, which is conducive to making high performance carbon fiber.

CONCLUSIONS

The P(AN-*co*-ABM) bipolymers used as precursor for carbon fiber were prepared by solution polymerization successfully, both the conversion of polymerization and molecular weight

Table VI. E_a determined by Kissinger and Ozawa Methods

Methods	Peak	PAN	ABM/AN = 0.0310	ABM/AN = 0.0491	ABM/AN = 0.0617	ABM/AN = 0.0761	ABM/AN = 0.0848
Kissinger	Peak1	168.39	93.47	86.80	98.99	92.64	98.92
	Peak 2		177.24	202.17	198.95	201.56	194.32
Ozawa	Peak 1	165.89	94.74	89.09	100.50	94.55	100.34
	Peak 2		174.02	197.20	195.87	196.88	190.68

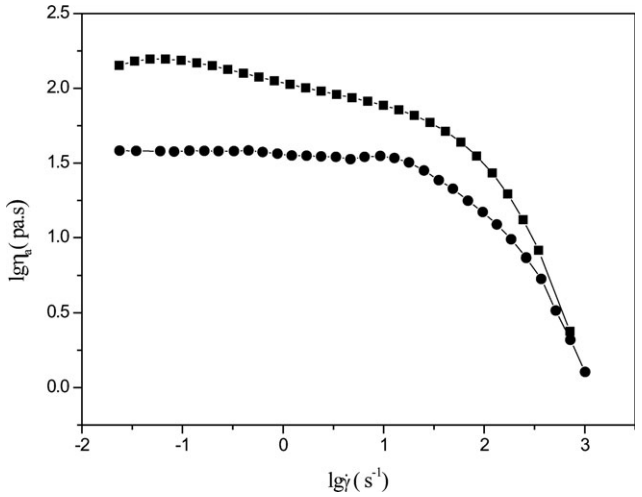

Figure 8. Plots of $\lg\eta_a$ versus $\lg\dot{\gamma}$ for PAN/DMSO and P(AN-*co*-ABM)/DSMO solutions at 70°C.

decrease with the increase of ABM amounts in the feed due to the large volume of MHI molecules. The AN/MHI reactivity ratios calculated by Fineman-Ross and Kelen-Tüdõs methods show good agreement and the reactivity ratios of ABM are larger than that of AN, which results in more ABM incorporated into polymer chains than AN. The cyclization of P(AN-*co*-ABM) can be initiated by bifunctional comonomer ABM through an ionic mechanism as evidenced from the appearance of two exothermic peaks in DSC curves. The P(AN-*co*-ABM) bipolymers show better stabilization than PAN homopolymer, such as lower initiation temperature and larger extent of stabilization under the same condition, which is mainly attributed to the ionic cyclization reactions induced by the bifunctional comonomer ABM. This is further confirmed by the calculation of E_a based on Kissinger method and Ozawa method. In addition, the rheological analysis shows that P(AN-*co*-ABM) possesses better spinnability than PAN, which is beneficial to the preparation of high performance carbon fiber.

ACKNOWLEDGMENTS

Financial support of this work from National Science Foundation of China (Grant Nos. 20971021, 51003013, 51073031, and 21171034) and innovation project of doctoral dissertation (No. BC2010-04) was gratefully acknowledged.

REFERENCES

1. Zhang, W. X.; Liu, J.; Wu, G. *Carbon* **2003**, *41*, 2805.
2. Shokuhfar, A.; Sedghi, A.; Eslami, F. R. *Mater. Sci. Tech.* **2006**, *22*, 1235.
3. Paris, O.; Loidl, D.; Peterlik, H. *Carbon* **2002**, *40*, 551.
4. Gupta, A. K.; Paliwal, D. K.; Bajaj, P. *Polym. Rev.* **1991**, *31*, 1.
5. Bahrami, S. H.; Bajaj, P.; Sen, K. *J. Appl. Polym. Sci.* **2003**, *89*, 1825.
6. Liu, J. J.; Ge, H. Y.; Wang, C. G. *J. Appl. Polym. Sci.* **2006**, *102*, 2175.
7. Devasia, R.; Reghunadhan, N. C. P.; Sadhana, R.; Babu, N. S.; Ninan, K. N. *J. Appl. Polym. Sci.* **2006**, *100*, 3055.
8. Devasia, R.; Reghunadhan, N. C. P.; Sivadasan, P.; Catherine, B. K.; Ninan, K. N. *J. Appl. Polym. Sci.* **2003**, *88*, 915.
9. Catta, P.; Sakata, S.; Garcia, G.; Zimmermann, J. P.; Galembeck, F.; Galembeck, F.; Giovedi, G. *J. Therm. Anal. Calorim.* **2007**, *87*, 657.
10. Chen, G. L.; Ju, A. Q.; Xu, H .Y.; Pan, D. *Polym. Mater. Sci. Eng.* **2010**, *26*, 146.
11. Devasia, R.; Reghunadhan, Na. C. P.; Ninan, K. N. *Polym. Int.* **2005**, *54*, 1110.
12. Chen, H.; Liang, Y.; Wang, C. Q. *J. Appl. Polym. Sci.* **2004**, *94*, 1151.
13. Gupta, V. B.; Kumar, S. *J. Appl. Polym. Sci.* **1981**, *26*, 1865.
14. Fineman, M.; Ross, S. D. *J. Polym. Sci.* **1950**, *5*, 259.
15. Kelen, T.; Tudos, F. *J. Macromol. Sci. Chem.* **1975**, *9*, 1.
16. Zhao, Y. Q.; Wang, C. G.; Wang, Y. X.; Zhu, B. *J. Appl. Polym. Sci.* **2009**, *111*, 3163.
17. Minagawa, M.; Miyano, K.; Takahashi, M.; Yoshii, F. *Macromolecules* **1988**, *21*, 2387.
18. Zhang, C.; Guang, S. Y.; Zhu, X. B.; Xu, H. Y.; Liu, X. Y.; Jiang, M. H. *J. Phys. Chem. C* **2010**, *114*, 22455.
19. Mittal, J.; Bahl, O. P.; Mathur, R. B.; Sandle, N. K. *Carbon* **1994**, *32*, 1133.
20. Patron, L.; Bastianelli, U. *Appl. Polym. Symp.* **1974**, *25*, 105.
21. Usami, T.; Itoh, T.; Ohtani, H.; Tsuge, S. *Macromolecules* **1990**, *23*, 2460.
22. Ouyang, Q.; Cheng, L.; Wang, H. J.; Li, K. X. *Polym. Degrad. Stab.* **2008**, *93*, 1415.
23. Yu, M. J.; Bai, Y. J.; Wang, C. G.; Xu, Y.; Guo, P. A. *Mater. Lett.* **2007**, *61*, 2292.
24. Xue, T. J.; Mckinney, M. A.; Wilkie, C. A. *Polym. Degrad. Stab.* **1997**, *58*, 193.
25. Bell, J. P.; Dumbleton. J. H. *Text Res. J.* **1971**, *41*, 196.
26. Bajaj, P.; Screekumar, T. V.; Sen. K. *Polymer* **2001**, *42*, 1707.
27. Wang, Y. X.; Liu, Y. l.; Wang, L. M.; Yang, Y. Z.; Wang, C. G. *e-Polymers* **2010**, *135*, 1.
28. Kissinger. H. E. *Anal. Chem.* **1957**, *29*, 1702.
29. Ozawa. T. *Bull. Chem. Soc. Jpn.* **1965**, *38*, 1881.
30. Jain, M. K.; Abhiraman, A. S. *J. Mater. Sci.* **1987**, *22*, 278.
31. Chiu, H. J.; Wang, Y. *J. Appl. Polym. Sci.* **1998**, *70*, 1009.
32. Wang, Y. D.; Wu. C. *J. Appl. Polym. Sci.* **1997**, *66*, 1389.
33. Zhou, Z.; Wu, X.; Wang. M. *Polym. Eng. Sci.* **1988**, *28*, 136.